G-actin regulates rapid induction of actin nucleation by mDia1 to restore cellular actin polymers

Chiharu Higashida[1], Shiro Suetsugu[2,3], Takahiro Tsuji[1], James Monypenny[1], Shuh Narumiya[1] and Naoki Watanabe[1,*]

[1]Department of Pharmacology, Kyoto University Faculty of Medicine, Yoshida Konoe-cho, Sakyo-ku, Kyoto 606-8501, Japan
[2]Laboratory of Membrane and Cytoskeleton Dynamics, Institute of Molecular and Cellular Biosciences, University of Tokyo, 1-1-1 Yayoi, Bunkyo-ku, Tokyo 113-0032, Japan
[3]Precursory Research for Embryonic Science and Technology (PRESTO), Japan Science and Technology Agency (JST), Honcho, Kawaguchi-shi, Saitama 332-0012, Japan
*Author for correspondence (e-mail: naoki-w@mfour.med.kyoto-u.ac.jp)

Accepted 15 July 2008
Journal of Cell Science 121, 3403-3412 Published by The Company of Biologists 2008
doi:10.1242/jcs.030940

Summary

mDia1 belongs to the formin family of proteins that share FH1 and FH2 domains. Although formins play a critical role in the formation of many actin-based cellular structures, the physiological regulation of formin-mediated actin assembly within the cell is still unknown. Here we show that cells possess an acute actin polymer restoration mechanism involving mDia1. By using single-molecule live-cell imaging, we found that several treatments including low-dose G-actin-sequestering drugs and unpolymerizable actin mutants activate mDia1 to initiate fast directional movement. The FH2 region, the core domain for actin nucleation, is sufficient to respond to latrunculin B (LatB) to increase its actin nucleation frequency. Simulation analysis revealed an unexpected paradoxical effect of LatB that leads to a several fold increase in free G-actin along with an increase in total G-actin. These results indicate that in cells, the actin nucleation frequency of mDia1 is enhanced not only by Rho, but also strongly through increased catalytic efficiency of the FH2 domain. Consistently, frequent actin nucleation by mDia1 was found around sites of vigorous actin disassembly. Another major actin nucleator, the Arp2/3 complex, was not affected by the G-actin increase induced by LatB. Taken together, we propose that transient accumulation of G-actin works as a cue to promote mDia1-catalyzed actin nucleation to execute rapid reassembly of actin filaments.

Supplementary material available online at
http://jcs.biologists.org/cgi/content/full/121/20/3403/DC1

Key words: Formin, mDia, G-actin, Rho, Actin nucleation

Introduction

Many actin-based cellular structures such as yeast actin cables, cytokinetic cleavage furrows and actin bundles in mammalian cells are dependent on formin family proteins (formins) (Evangelista et al., 2003). FH2 or FH1-FH2 domains nucleate actin filaments (Pruyne et al., 2002; Sagot et al., 2002) and they processively remain associated with the growing barbed-end of filaments (Higashida et al., 2004; Kovar et al., 2006; Romero et al., 2004; Zigmond et al., 2003). However, the physiological regulation of formin-mediated actin assembly, both temporally and spatially within the cell, is still unknown.

mDia1 is regulated by the autoinhibitory interaction between the GTPase-binding domain (GBD) within its N-terminus and the diaphanous autoregulated domain (DAD) within its C-terminus (Li and Higgs, 2003; Rose et al., 2005; Watanabe et al., 1999). RhoA, RhoB and RhoC bind to its N-terminal GBD and reduce the autoinhibitory interaction between GBD and DAD. This activation of mDia1 exposes its FH1-FH2 region, which can then nucleate actin filaments, and accelerate the rate of actin elongation 5- to 15-fold (Kovar et al., 2006; Romero et al., 2004). The marked loss of actin fibers and the cytokinetic contractile ring in cells treated with *Clostridium botulinum* C3 exoenzyme (C3), which specifically inactivates Rho, suggests a major role for Rho-mDia signaling in the generation and maintenance of cellular actin polymers (Mabuchi et al., 1993; Ridley and Hall, 1992).

We have previously elucidated the processive actin-capping property of the FH1-FH2 domain by observing single molecules of mDia1 expressed at low levels in live XTC fibroblasts (Higashida et al., 2004). An FH1-FH2 domain mutant of mDia1, mDia1ΔN3, fused to an enhanced green fluorescent protein (EGFP) exhibits fast directional movement, and is processively associated with the growing barbed ends of filaments. In contrast to mDia1ΔN3, full-length mDia1 fused to EGFP (EGFP-mDia1Full) hardly exhibits processive movement, presumably because of the autoinhibitory intramolecular interaction. We observed rapid induction of processive movement of mDia1Full by microinjecting recombinant RhoA-Val14 (Higashida et al., 2004). Thus, molecular imaging (Miyoshi et al., 2006; Watanabe and Mitchison, 2002) is a potent tool to visualize the site of action of formins. For example, the yeast formins For3p and Bni1p transiently appear at the cell tip, then nonpolymerizing For3p and Bni1p are carried away towards the center of the cell by the retrograde flow of actin filaments (Buttery et al., 2007; Martin and Chang, 2006). Therefore, yeast formins might transiently assemble actin cables at the cell tip, but it is still unclear how the processive actin assembly mechanism of formins is regulated within the cell.

Here we report that a transient increase in free G-actin efficiently promotes mDia1-catalyzed actin nucleation in cells. By using single-molecule live-cell imaging, we found that low-dose G-actin-sequestering drugs, such as LatB, rapidly induce processive

movement of wild-type mDia1 as well as mDia1 mutants consisting of the FH2 region, the core domain for actin nucleation. Taking F-actin turnover into account, our simulation analysis estimates that low-dose LatB treatment could lead to a paradoxical several fold increase in free G-actin. These results suggest that in cells, mDia1 is converted to the processive actin assembly state not only by Rho, but also through an increased catalytic efficiency of the FH2 domain. We also present physiological evidence for G-actin regulation of mDia1-catalyzed actin nucleation. mDia1 speckles frequently appear around the sites of vigorous actin disassembly. Furthermore, actin nucleation by another formin, FRL1, is also promoted by low-dose LatB treatment whereas the Arp2/3 complex, which is a major actin nucleator, is not. Actin nucleators are probably regulated differentially by fluctuation of the free G-actin concentration. Taken together, we propose that transient accumulation of G-actin works as a cue to promote mDia1-catalyzed actin nucleation to restore loss of actin filaments in the cell.

Results

The behavior of wild-type mDia1 observed by single-molecule imaging

We first investigated the behavior of mDia1Full under normal conditions. Although the fluorescence signal from EGFP-mDia1Full was distributed diffusely throughout the cytoplasm, mDia1Full occasionally appeared as a discrete spot. The fluorescence intensity was comparable to around two molecules of single-molecule EGFP-actin (Watanabe and Mitchison, 2002). mDia1 is known to form a dimer (Li and Higgs, 2003; Rose et al., 2005). We classified these discrete signals of EGFP-mDia1Full, which we call 'speckles', into four groups; processive (4.3±3.6%), random (24.8±13.7%), stationary (47.5±14.6%) and unclassified (23.4±14.0%) (Fig. 1A,B; supplementary material Fig. S1A). Processively moving speckles are those that could be traced for at least five consecutive images in one direction. Although they represent a minor population, they serve as the best measure of mDia1 functions related to actin assembly. Stationary mDia1 tethered to cell structures may possibly bind growing actin barbed ends. However, growth of such barbed ends should occur slowly because of crosslinking of F-actin in animal cells. Indeed, the rate of retrograde flow (0.014 μm/second; measured by tropomyosin-EGFP) was more than 60 times slower than the rate of processive movement of mPlum-mDia1ΔN3 (0.88 μm/second). There were no obvious tropomyosin speckles moving at a similar speed to mDia1ΔN3 (supplementary material Movie 1). We therefore predict that the majority of mDia1-mediated actin assembly is provided by the processive group.

In agreement with our previous observations using microinjection of recombinant RhoA-Val14 (Higashida et al., 2004), processive mDia1Full speckles were also induced by coexpression of RhoA-Val14. Conversely, processive movement is inhibited by C3. Normalized frequency (the number of processive speckles divided by total intensity of EGFP fluorescence in the measured region) of mDia1 processive speckles in C3-treated cells, in control cells and in RhoA-Val14 expressing cells are 0, 2.26±4.35 and 35.4±12.7, respectively (a.u., mean ± s.d., n=6 cells; for control and C3-treated cells; n=7 cells for RhoA-Val14 cells). The average speed of mDia1Full was 1.7 μm/second in RhoA-Val14 expressing cells. These data further support our measurement of processive mDia1Full speckles as a tool to detect the spatiotemporal regulation of Rho-mDia1 signaling.

Random speckles displayed movement that involved frequent changes in orientation and speed (Fig. 1A). We currently do not know the function of randomly moving speckles with respect to the regulation of mDia1. Nonetheless, the movement of random speckles was independent of actin polymerization because it was still observed under the conditions where actin elongation was completely inhibited (Higashida et al., 2004) by 1 μM latrunculin B (LatB) (Coue et al., 1987) or 1 μM cytochalasin D (CytD) (Sampath and Pollard, 1991) (Fig. 1C). The unclassified group covers all speckles that could not be traced over five consecutive images. We therefore focused on the processive group to elucidate the activation state of mDia1.

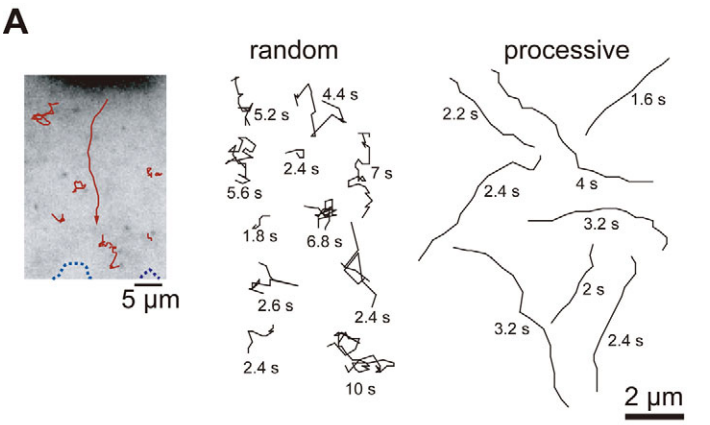

B

classification	processive	random	stationary	unclassified
percentage (mean ± s.d.)	4.3±3.6	24.8±13.7	47.5±14.6	23.4±14.0

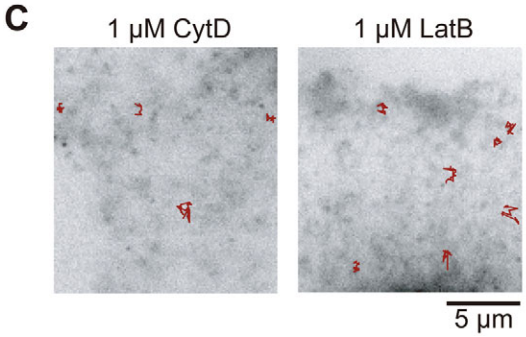

Fig. 1. The behavior of wild-type mDia1 in XTC cells. (A) Single-molecule imaging of EGFP-mDia1Full speckles reveals different types of motility. Red lines show trajectories of mDia1Full speckles observed within a 6 second time window. Blue dotted lines indicate the contour of the cell edge (left). Representative trajectories of random (middle) and processive (right) mDia1Full speckles are shown. (B) mDia1Full speckles found within a 6 second time window are classified into the indicated groups (n=11 cells) as described within the text. (C) Motility of mDia1Full speckles in the random group is independent of actin polymerization. Random speckles were still observed 1 minute after 1 μM CytD or 1 μM LatB treatment. Trajectories of mDia1Full speckles found within a 6 second time window are shown.

Actin-monomer-sequestering drugs induce appearance of processive mDia1

In the present study, we sought cellular conditions where directional movement of mDia1 is induced frequently. Interestingly, we found that treatment with a low dose of LatB (100 nM) induces processive movement of mDia1Full. mDia1Full speckles were frequently observed as early as 10 seconds after the perfusion of 100 nM LatB (Fig. 2A; supplementary material Movie 2). The number of processively moving speckles markedly increased over time (Fig. 2B). Both the total number of mDia1 speckles and the fraction of processively moving speckles increased 3.8 and 5.7 times (from 9.6% to 54.7%) 100 seconds after perfusion, respectively (supplementary material Fig. S1B). LatB reduces the concentration of polymerization-competent monomers by binding to G-actin, but at 100 nM, the reduction in the speed of processively moving mDia1 speckles occurs slowly, allowing us to observe them over time. Even 100 seconds after treatment, mDia1Full speckles (0.131 μm/second) (Fig. 2B) moved more than five times faster than the actin flow at the cell periphery (0.025 μm/second) (Watanabe and Mitchison, 2002). The most frequent processive movement of mDia1 at 100 seconds was observed at 80 nM. Even 30 nM LatB was found to induce some movement (Fig. 2C).

Although 100 nM LatB is able to disassemble F-actin gradually, activation of mDia1Full seemed to occur faster than the apparent actin structure disruption. We observed a gradual loss in the F-actin signals but actin structures were not corrupted even 100 seconds after perfusion of 100 nM LatB (Fig. 2D). To exclude the possibility that LatB treatment induced processive mDia1 movement by increasing barbed ends, we monitored single-molecule speckles of capping protein (CAPZB) (Miyoshi et al., 2006). The number of capping protein speckles did not increase upon treatment with 100 nM LatB (Fig. 2E; supplementary material Movie 3). We also quantified free barbed ends by measuring incorporation of Rhodamine-labeled actin after permeabilization. Although free barbed ends redistributed from the periphery to the central region of cells upon 100 nM LatB treatment, the total amount of free barbed ends did not change significantly (supplementary material Fig. S2).

We also tested swinholide A (SwinA), which inhibits actin polymerization by sequestering G-actin as a dimer (Bubb et al.,

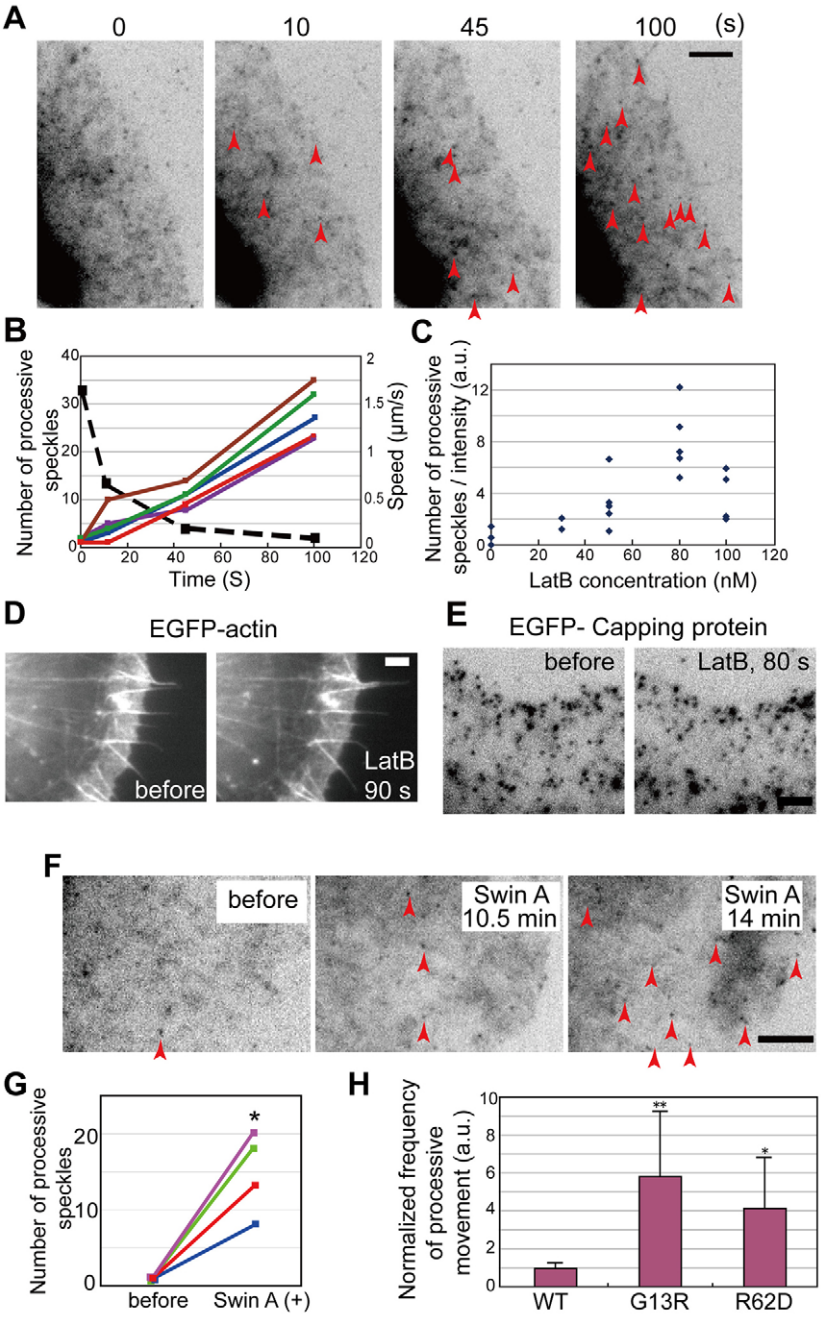

Fig. 2. Latrunculin B at low dose induces processive movement of mDia1. (A) Processive movement of EGFP-mDia1Full was induced after 100 nM LatB perfusion. Arrowheads indicate mDia1Full speckles moving processively at indicated time points. Marked speckles moved in one direction for at least five consecutive frames. Scale bar: 5 μm. (B) Number of speckles moving processively after perfusion with 100 nM LatB. Each colored line indicates data from an individual cell. Dotted black line indicates the average speed of processive speckles in five cells. (C) Normalized frequency of processive mDia1 speckles in cells treated with various concentrations of LatB for 100 seconds. Normalized frequency was calculated by dividing the number of speckles by total intensity of EGFP fluorescence in the imaged region. (D) F-actin structures were well preserved 90 seconds after 100 nM LatB treatment except for a gradual loss in the EGFP-actin signal (12%) in the lamellipodial actin meshwork. Scale bar: 5 μm. (E) The density of capping protein speckles (EGFP-CPβ1) did not change before and 80 seconds after 100 nM LatB treatment. Scale bar, 2 μm. (F) Treatment of EGFP-mDia1Full expressing cells with 500 nM SwinA. Arrowheads indicate mDia1Full speckles moving processively. Scale bar: 5 μm. (G) The number of processive mDia1Full speckles before and 11 minutes after 500 nM SwinA perfusion. Data were analyzed using a two-tailed Student's *t*-test. $*P<0.02$. (H) Flag-tagged actins, WT (wild-type), R62D or G13R, were coexpressed with EGFP-mDia1Full. Normalized frequency of processive mDia1 speckles in cells expressing actin WT, R62D or G13R is shown. Data were normalized by dividing the number of processive speckles by total intensity of EGFP fluorescence in the imaged region (mean ± s.d., $n=5$ cells for WT; $n=12$ cells for G13R; $n=16$ cells for R62D) and analyzed using a two-tailed Student's *t*-test. $*P<0.02$; $**P<0.01$.

1995). The number of processively moving mDia1Full speckles increased after treatment with 500 nM SwinA (Fig. 2F,G; supplementary material Movie 4). Various concentrations of jasplakinolide, which stabilizes F-actin (Bubb et al., 1994), did not increase the number of processively moving speckles (data not shown).

These results indicate that treatment with LatB or SwinA induces processively moving mDia1, and this induction occurs without marked disruption of actin stress fibers. We therefore speculated that an increase in the unpolymerized actin monomer concentration may lead to an increase in the actin nucleation frequency by mDia1.

To test this, we expressed Flag-tagged wild-type actin and nonpolymerizable actin mutants (Posern et al., 2002) with EGFP-mDia1Full. Both of the Flag-tagged mutant actins increased the number of processively moving mDia1Full speckles, whereas Flag-tagged wild-type actin did not (Fig. 2H; supplementary material Fig. S3 and Movie 5). Immunostaining (supplementary material Fig. S3A) revealed that although wild-type actin was incorporated into F-actin structures, the R62D and G13R mutants showed diffuse localization within the cytoplasm. Frequent induction of processively moving mDia1 speckles was observed without an apparent change of F-actin structures in cells expressing R62D or G13R actin (supplementary material Fig. S3B).

Normally, cells contain a pool of G-actin bound to profilin and sequestering proteins such as thymosin-β4, leaving the free G-actin concentration very low (Pollard et al., 2000). Free G-actin may not exist at a high concentration because it may lead to spontaneous nucleation and transfer of free G-actin to F-actin. These results (Fig. 2) suggested that accumulation of a certain state of G-actin, either LatB-bound or unbound, caused frequent induction of processively moving mDia1 speckles.

FH2 region is sufficient for the induction of processive movement by LatB

We next examined whether the observed induction of processively moving mDia1 speckles was dependent upon Rho activity. We introduced C3 into cells using electroporation (Fig. 3A) (Kato et al., 2001) and found that C3 inhibited processive movement of mDia1 induced by 100 nM LatB (Fig. 3B,C; supplementary material Movie 6).

Although these results suggested that Rho mediates the induction of processive mDia1 movement by LatB, we found that the FH1-FH2 or FH2 region of mDia1 alone can be affected by low-dose LatB (Fig. 3D; supplementary material Movies 7 and 8). In contrast to mDia1Full, the induction of processive speckles

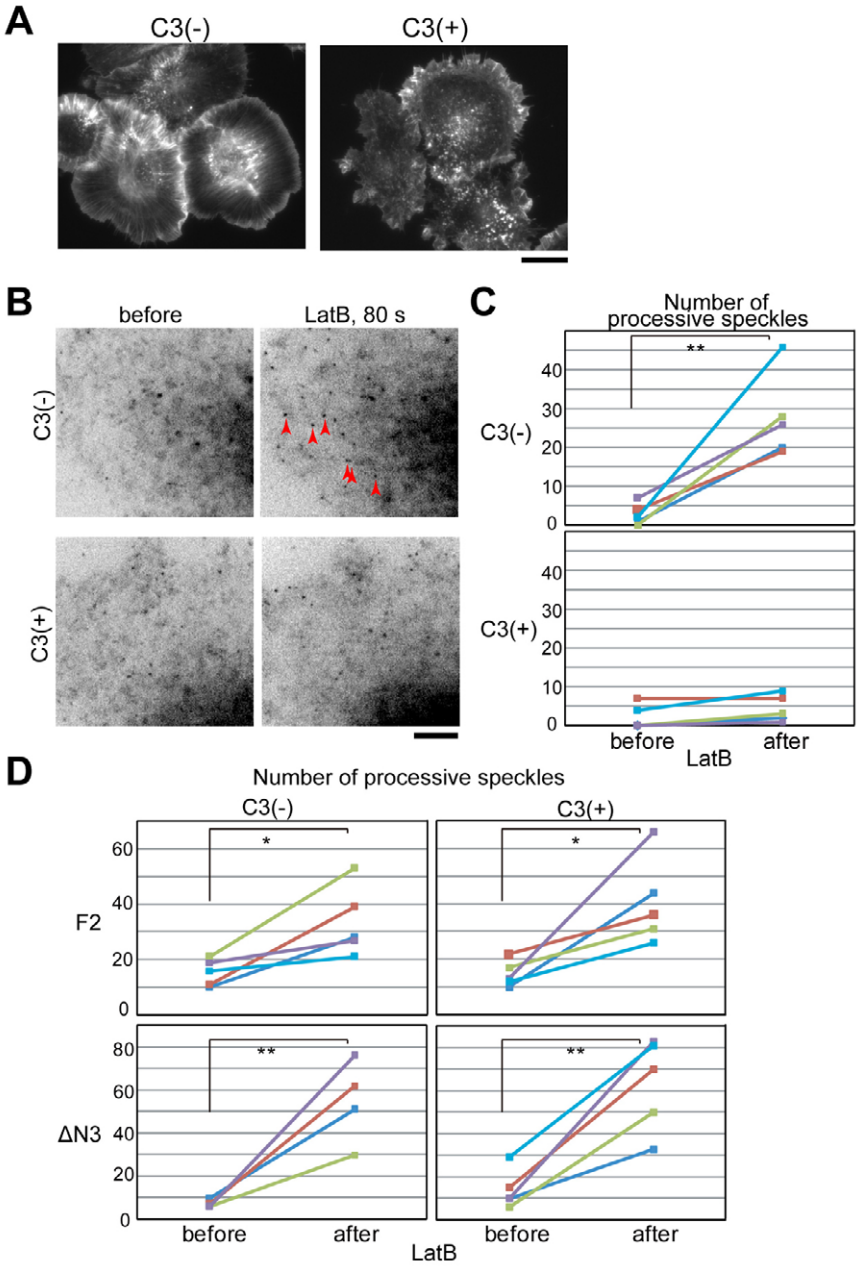

Fig. 3. Rho is required, but the FH2 region is sufficient for processive movement induced by LatB. (A) Cells were electroporated in the presence (right) or absence (left) of C3-exoenzyme and allowed to spread on the PLL-coated glass coverslips for 30 minutes. Phalloidin staining shows the loss of actin stress fibers in C3-treated cells indicating the efficient incorporation of C3-exoenzyme. Scale bar: 20 μm. (B) Cells expressing EGFP-mDia1Full were electroporated in the presence (lower panels) or absence (upper panels) of C3. Then time-lapse images were taken before and 80 seconds after treatment with 100 nM LatB. Arrowheads indicate processively moving mDia1Full speckles. Scale bar: 5 μm. (C) The number of processive mDia1Full speckles in the electroporated cells was counted before and 100 seconds after 100 nM LatB perfusion. The same area within each cell was used for measurement before and after the LatB treatment. C3 inhibited the induction of processive speckles by LatB. (n=5 cells; $^{**}P<0.01$, two-tailed paired t-test.) (D) A low dose of LatB increases the number of processive speckles of the FH2 region mutant (mDia1F2) and the FH1-FH2 region mutant (mDia1ΔN3) in a C3-insensitive manner. Cells expressing EGFP-mDia1F2 or EGFP-mDia1ΔN3 were electroporated in the presence or absence of C3. For mDia1F2, speckles were counted before and 50 seconds after 50 nM LatB perfusion. For EGFP-mDia1ΔN3, speckles were counted before and 80 seconds after 100 nM LatB perfusion. The same area within each cell was used for the measurement. ($^{*}P<0.03$ and $^{**}P<0.005$, two-tailed paired t-test.) Since the measured cell areas are different, the number of processive speckles is not comparable between different constructs.

of the FH1-FH2 or FH2 mutant of mDia1 by LatB was not inhibited by C3 (Fig. 3D). These results suggest that LatB treatment increases the actin nucleation frequency of mDia1 through its catalytic domain and apart from the release of autoinhibition of mDia1 induced by Rho binding. Our data indicate that Rho is required for mDia1 to be in an open conformation but is not a direct mediator of LatB-induced frequent actin nucleation by mDia1.

Increase in free G-actin possibly triggers frequent actin nucleation by mDia1

Since the FH2 core domain responded to LatB treatment (Fig. 3D) and FH2-catalyzed nucleation is promoted by free G-actin but not by the profilin-actin complex (Li and Higgs, 2003; Paul and Pollard, 2008), we examined whether LatB-bound actin might contribute to mDia1FH2-catalyzed nucleation. Under the conditions tested in vitro, LatB inhibited mDia1FH2-mediated actin filament assembly in a concentration-dependent manner (Fig. 4A; supplementary material Fig. S4A). In addition, LatB did not promote mDia1FH2-mediated actin filament assembly in the presence of profilin (supplementary material Fig. S4B).

We then wondered whether low-dose LatB treatment might increase the cellular concentration of free G-actin. LatB competes with thymosin-β4 binding to G-actin (Yarmola et al., 2000). A previous study has estimated that free G-actin does not change upon treatment with 100 nM latrunculin A (LatA) despite accumulation of this drug in the neutrophil cytoplasm (Pring et al., 2002). The authors concluded that an unknown mechanism might be required to explain the impaired migration of neutrophils treated with 100 nM LatA. We re-evaluated this issue by building a kinetic model that incorporates our observation of a decrease in actin assembly upon 100 nM LatB treatment (Fig. 2B; see supplementary material Fig. S5 for detail). Only two G-actin-sequestering proteins, profilin and thymosin-β4, were considered. Given their abundance, we presume that the effect of other minor G-actin-binding proteins can largely be represented by two proteins with different competitiveness against LatB. To our surprise, it was found that free G-actin increases several fold within 2 minutes (Fig. 4B). We also checked the effect of different ratios and affinities between actin and G-actin and overall F-actin turnover rates on the free G-actin concentration in a simulation analysis. Within a reasonable range of parameters, we consistently observed increases in free G-actin (supplementary material Fig. S5A-E), and these increases were in good agreement with the time course of the increase in the number of processively moving mDia1Full speckles (Fig. 2B). Note that the increase in free G-actin occurs in the presence of LatB accumulation in the cytoplasm at ~5 μM (Fig. 4B, right).

Modulation of actin filament turnover by LatB is the key for the induction of this paradoxical increase of G-actin. Without the G-actin supply due to imbalance between actin assembly and disassembly, the free G-actin increase is not induced (supplementary material Fig. S5A, the curve for the F-actin turnover rate of 0 second^{-1}). This observation is consistent with a previous report estimating a negligible change in the free G-actin concentration in neutrophils treated with 100 nM LatA (Pring et al., 2002). In this report, the

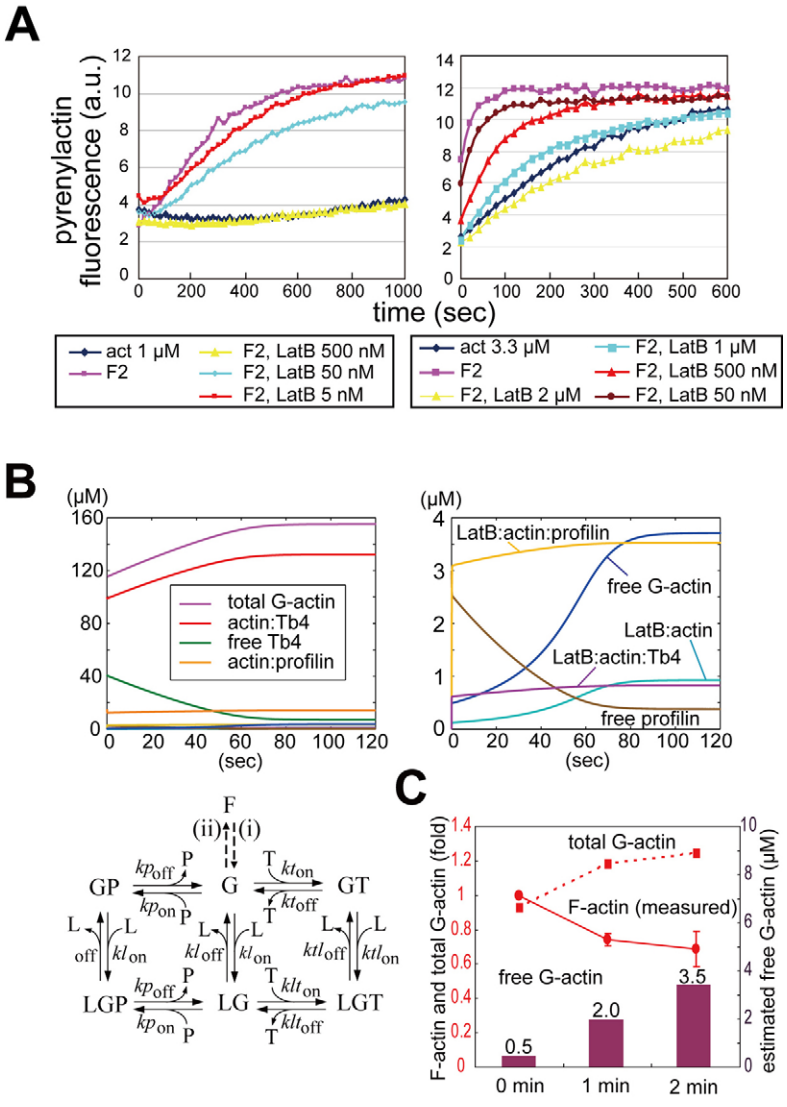

Fig. 4. LatB treatment paradoxically increases free G-actin concentration in the cell. (A) Effects of LatB on actin polymerization mediated by mDia1F2. Representative results showing no obvious promoting effect of LatB on mDia1F2-induced actin assembly. Actin (1 μM, left panel; 3.3 μM, right panel; 20% pyrene labeled) was polymerized in the presence of various concentrations of LatB with 21.8 nM (left) or 10 nM (right) mDia1F2. (B) Simulation analysis reveals a paradoxical increase in free G-actin upon low-dose LatB treatment. This kinetic model (bottom) concerns changes in the concentration of G-actin (G), either free or bound to thymosin-β4 (T), profilin (P) and LatB (L). The graphs show simulation at 0.1 μM LatB, 0.5 μM free G-actin at t=0, 115.5 μM total G-actin at t=0, 240 μM total actin, 140 μM total thymosin-β4 (40 μM free Tb4 at t=0) and 18 μM total profilin (3 μM free profilin at t=0). On the right, curves for five parameters are enlarged. Note the rapid increase in free G-actin despite the accumulation of LatB to ~5 μM in the cytoplasm. (C) Estimation of the equilibrium state also predicts an increase in free G-actin. Relative F-actin contents were quantified by phalloidin binding in cells treated with 100 nM LatB for 0, 1 and 2 minutes (line, mean ± s.d. of three separate experiments; n=275 cells, n=245 cells and n=201 cells, respectively). Dashed line and columns show changes in total G-actin and free G-actin, respectively, estimated by calculating the equilibrium state between G-actin and its interacting molecules based on the observed F-actin decrease.

change in the ratio between G-actin and F-actin was not considered. Our improved model predicts that only a ~30% increase in the total G-actin is required to induce the several fold increase in free G-actin.

Since the currently available assays are not sensitive enough to distinguish free G-actin from G-actin bound to monomer-binding proteins that are abundant in cells, we measured the change in F-actin during LatB treatment instead. We show further evidence of the LatB-induced free G-actin increase using a different calculation method from the above simulation (Fig. 4B). First, we found that the amount of cellular F-actin was reduced by 25.7% and 31.3%, 1 and 2 minutes after 100 nM LatB perfusion, respectively (Fig. 4C). Using the same approach as the previous study (Pring et al., 2002), which calculates the equilibrium state between G-actin and its binding molecules, we estimated the concentration of total G-actin and free G-actin from the observed F-actin decrease. This calculation based on the different observation again predicts increases in free G-actin to 2.0 and 3.5 μM at 1 and 2 minutes, respectively (Fig. 4C). The estimated concentrations of G-actin species either free or bound to LatB, thymosin β4 or profilin are shown in supplementary material Fig. S5F.

Our simulations predict that cells should be resistant to a loss in F-actin induced by LatB if they contain high concentrations of actin filament nucleators regulated by the concentration of G-actin (large constant *C*, supplementary material Fig. S5B). We examined the effect of overexpressed mDia1 on total F-actin amounts before and after low-dose LatB treatment. Cells overexpressing mDia1Full retained not only actin stress fibers but also thin F-actin structures throughout the cytoplasm (Fig. 5A). Low-dose LatB significantly decreased F-actin in nontransfected cells, but not in cells overexpressing mDia1Full (Fig. 5B). Thus, overexpressed mDia1 suppresses the F-actin decrease induced by low-dose LatB treatment, supporting the role of mDia1 in restoration of cellular actin polymers.

Frequent appearance of processive mDia1 around sites of vigorous actin disassembly

We sought to determine the physiological role of enhanced nucleation activity of mDia1 upon the increase of G-actin. Observation of mDia1F2 time-lapse imaging revealed that mDia1F2 speckles frequently emerged around specific foci near the boundary between lamellipodia and the lamellae region (Fig. 6A). These foci for frequent mDia1F2 appearance were dynamically associated with AIP1, a cofilin-interacting protein (Fig. 6A,B; supplementary material Movie 9). mDia1Full speckles also appeared at a higher frequency in areas labeled densely by mPlum-AIP1 (Fig. 6C). We observed the identical localization and dynamics of AIP1 and XAC2 (Abe et al., 1996), a *Xenopus* cofilin, at the cell periphery using immunostaining and live cell imaging (supplementary material Fig. S6). AIP1 cooperates with cofilin to disassemble actin filaments in vitro (Brieher et al., 2006; Ono, 2003).

Although the precise mechanism of cooperation between cofilin and AIP1 is not fully understood, promotion of cofilin-induced filament severing by AIP1 may augment depolymerization. In vitro, AIP1 binds actin barbed ends in a manner that is highly dependent on cofilin (Ono, 2003), which could lead to an increase in pointed ends. In cells, the activity of cofilin plays an essential role in actin disassembly (Hotulainen et al., 2005; Miyoshi et al., 2006) and in the interaction of AIP1 with F-actin (T.T. and N.W., unpublished observations). We therefore used mPlum-AIP1 as a marker for the site of fast actin disassembly. The results are consistent with our idea that mDia1 increases its actin nucleation efficiency around the sites undergoing fast actin disassembly under physiological conditions.

G-actin increase promotes actin nucleation by FRL1 but not Arp2/3 complex

We tested whether behavior of other nucleation-promoting factors might be affected by low-dose LatB treatment. Processively moving speckles of FRL1 (formin-related gene in leukocytes) significantly increased after 100 nM LatB treatment (Fig. 7A; supplementary material Movie 10). By contrast, the density of speckles of p40, a subunit of the Arp2/3 complex (Miyoshi et al., 2006), did not increase upon LatB treatment (Fig. 7B). mDia1 and FRL1 may thus effectively nucleate actin filaments in response to a G-actin increase whereas the Arp2/3 complex might react less efficiently to the change in G-actin concentration. The activity of actin nucleators might be regulated differentially by the G-actin concentration in cells.

Discussion

We propose that cells possess an acute actin polymer assembly mechanism involving mDia1. We found that induction of processive mDia1speckles occurs within 10 seconds upon treatment with LatB, an actin-monomer-sequestering drug. In addition, mDia1 activation occurred without marked

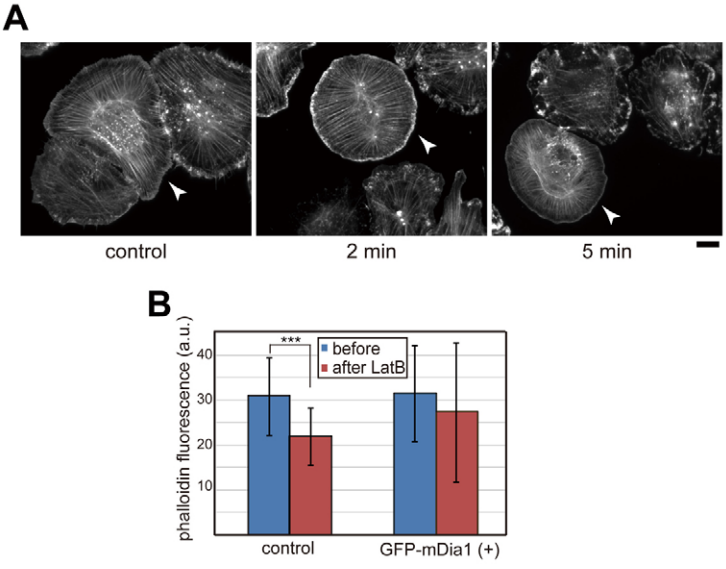

Fig. 5. Overexpression of mDia1Full prevents F-actin disassembly induced by low-dose LatB treatment. (A) F-actin structures visualized by fluorescent phalloidin before and after 100 nM LatB treatment. Note the well preserved thin actin fiber architecture in cells overexpressing EGFP-mDia1Full (arrowheads), whereas F-actin structures were gradually disrupted in nontransfected cells. Scale bar: 10 μm. (B) Cells transfected with pEGFP-mDia1Full were fixed and stained with fluorescent phalloidin before and 8 minutes after 50 nM LatB treatment. Total intensity of the phalloidin signal was measured in each transfected and nontransfected cell. F-actin did not decrease significantly in EGFP-mDia1-expressing cells [mean ± s.d.; non-transfected cells, n=143 (before), n=265 (after); EGFP-mDia1 positive cells, n=42 (before), n=53 (after)]. Data were analyzed using a two-tailed Student's t-test; ***P<0.001.

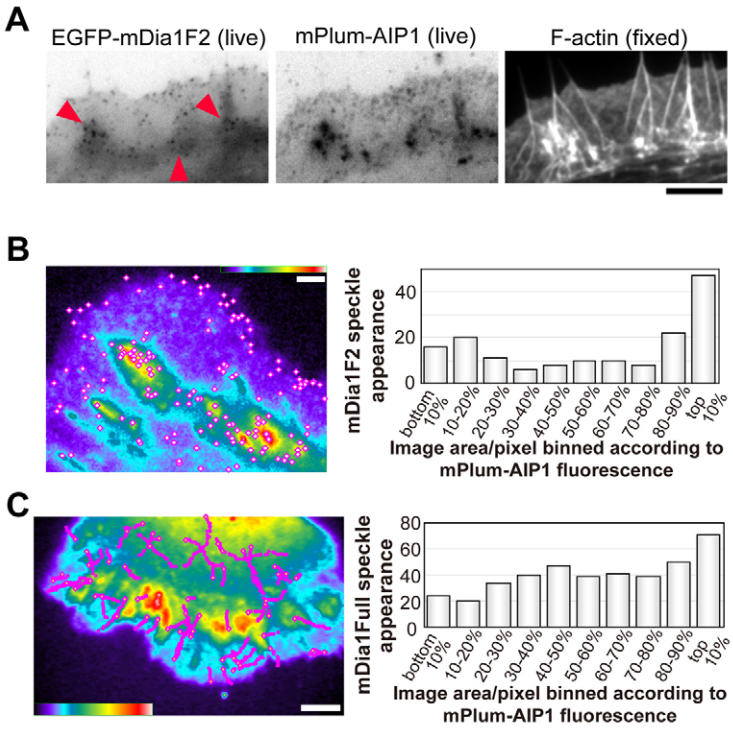

Fig. 6. Frequent actin nucleation by mDia1 around sites of vigorous actin disassembly. (A) Images of EGFP-mDia1F2 (left) and mPlum-AIP1 (middle) were acquired in a live cell. Cells were then fixed, and stained with phalloidin in order to visualize F-actin (right). Note the clusters of mDia1F2 speckles (arrowheads) around the area labeled strongly with AIP1, a cofactor of cofilin. (B,C) Frequency of mDia1 speckle appearance is biased toward the region of high AIP1 concentration. The images show the position of mDia1F2 appearance (B, diamonds) or mDia1Full speckle appearance (C, white dots), mDia1Full trajectories (C, pink circles) and the intensity of mPlum-AIP1 fluorescence (pseudocolor). In the graphs, the x, y position of individual pixels within an mPlum-AIP1 image was binned into ten equal areas according to their fluorescence intensity values. Intensity-sorted positions were then used to correlate the appearance of mDia1 speckles with the local intensity of mPlum-AIP1 fluorescence (B, n=158, 1 cell; C, n=405, 11 cells). mDia1F2 speckles frequently emerged in areas strongly labeled with mPlum-AIP1. Frequency of mDia1Full speckle appearance shows positive correlation with the intensity of mPlum-AIP1 (P<0.01). Scale bars: 5 µm.

disruption in F-actin structures in the LatB-treated cells and in cells expressing G13R and R62D actin mutants. The association of capping protein with F-actin did not increase upon treatment with 100 nM LatB. Free barbed ends quantified in permeabilized cells did not change upon LatB treatment. It is therefore unlikely that induction of processive mDia1 speckles by LatB was due to an increase in free barbed ends. Our results using two calculations based on distinct observations estimate a paradoxical increase in free G-actin in LatB-treated cells. We therefore propose that an increase in G-actin works as a cue to increase the frequency of actin nucleation by mDia1.

Our current estimation of the free G-actin concentration may not be very accurate because of the lack of precise information on parameters such as the total cellular actin nucleation activities in the kinetic modeling (Fig. 4B) and the effects of minor G-actin-binding proteins in the equilibrium calculation (Fig. 4C). The estimated fold increase in free G-actin could vary depending on parameter values (supplementary material Fig. S5). Additionally, an estimated parameter that is complicated in our measurements is the concentration of the LatB-free profilin:actin complex. Its estimated concentration remained 70-80% of the initial value whereas we observed a rapid >60% reduction in the speed of mDia1Full speckles after LatB treatment. Nevertheless, our simulation analysis revealed a previously unnoticed relationship between free G-actin and the G-actin:F-actin ratio. In this regard, it is important to note that a 3.8-fold change in free G-actin has

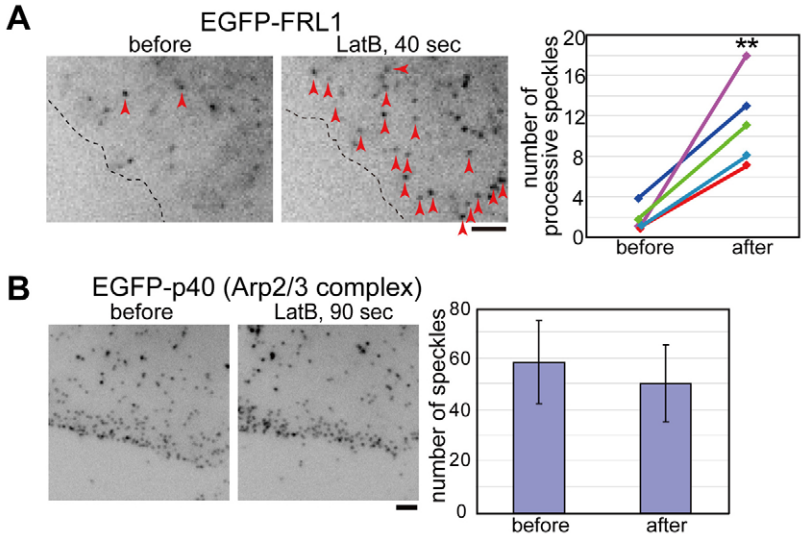

Fig. 7. Effects of low-dose LatB on the activity of other actin nucleators. (A) Processive movement of EGFP-FRL1 was induced 40 seconds after 100 nM LatB perfusion. Arrowheads indicate FRL1 speckles moving processively. Owing to the decrease in speed, the speckles that moved in one direction for at least seven consecutive frames are labeled as processive after LatB treatment. Dotted lines indicate cell contour. The graph shows the number of EGFP-FRL1 speckles moving processively before and 50 seconds after treatment. Each colored line represents data from an individual cell. Data were analyzed using a two-tailed paired t-test; **P<0.01. (B) No obvious change in the density of speckles of the Arp2/3 complex was observed after 100 nM LatB treatment. Images were taken before and 90 seconds after treatment. The graph shows the number of single-molecule EGFP-p40 speckles before and 90 seconds after treatment (mean ± s.d., n=5 cells). The areas devoid of densely packed speckles were used for analysis. The loss of EGFP-p40 signal between the two conditions as a result of photobleaching is less than 10%. Scale bars: 2 µm.

also been estimated based on the different amounts of F-actin in stimulated and unstimulated leukocytes (Pring et al., 2002). Hence, we and Pring et al. consistently predict several-fold free G-actin increases associated with the increased G-actin:F-actin ratio. We strongly believe that at least qualitatively, our results using two estimations based on different observations (Fig. 4B,C), provide compelling evidence that in low-dose LatB perfusion experiments, processive movement of mDia1 could be triggered by an increase in free G-actin. Our results also highlight an unprecedented case in which an antagonist may increase the concentration of drug-free targets in a complex biological system.

To be mobilized by LatB treatment, mDia1 requires Rho activity, but the FH2 region is sufficient. Rho signaling presumably determines the ratio of the opened and closed form of mDia1 within the cell. Once opened, a G-actin increase initiates actin nucleation by mDia1, leading to fast, long-range actin filament assembly. Previously, Rho binding and subsequent release from autoinhibition have been thought to be the major regulatory mechanism of mDia1 activation. Our data revealed that apart from the elevated amount of activated Rho, mDia1 may be efficiently converted to the actin-nucleating state through its catalytic domain by sensing a G-actin increase.

Our data (Fig. 2F,G) also show the remarkable induction of processive mDia1 speckles by treatments analogous to LatB. How might SwinA and unpolymerizable actins promote the appearance of processive mDia1 speckles? SwinA sequesters actin as a dimer. G-actin crosslinked in the presence of SwinA forms an anti-parallel dimer (Bubb et al., 1995). This dimer species is distinct from a readily polymerizing dimer obtained by crosslinking adjacent subunits in the F-actin helix (Millonig et al., 1988). The SwinA-induced antiparallel dimer does not fit with the structure of actin in complex with the FH2 domain of Bni1p (Otomo et al., 2005), nor does it promote actin nucleation (Millonig et al., 1988). Therefore, direct promotion of nuclei formation by SwinA is unlikely. We postulate that SwinA may induce frequent mDia1-catalyzed actin nucleation by increasing free G-actin in a manner that is similar to LatB.

With regard to actin mutants, there might be two mechanisms. One is direct participation of mutant actins in the nucleation step. Preliminary results showed that both Flag-tagged G13R and R62D actins bind endogenous actin in an immunoprecipitation assay using anti-Flag antibodies (Hiroyuki Miyoshi, Kyoto University, personal communication), although G13R actin does not bind wild-type actin in a yeast two-hybrid assay (Posern et al., 2002). Therefore, despite their inability to copolymerize with cellular F-actin, G13R and R62D actins retain an ability to interact with native actin in the soluble form. Alternatively, overexpresssion of mutant actins may increase free G-actin by occupying G-actin-sequestering proteins. Our simulation analysis (supplementary material Fig. S5C) shows that as the amount of G-actin-sequestering proteins comes close to that of G-actin, more G-actin is released from its partners. Actin R62D binds cofilin but not profilin (Posern et al., 2004). Actin G13R interacts with profilin and not with cofilin in a two-hybrid assay (Posern et al., 2002). Thus, it is possible that mutant actins increase free G-actin by occupying G-actin-sequestering proteins. In addition, two mutant actins attenuate the activity of the serum response factor (Posern et al., 2002). However, this could lead to a decrease rather than an increase in endogenous actin. Hence involvement of the transcriptional regulation of the gene encoding actin is less likely. Further analysis is required to elucidate the precise mechanisms for the induction of processive mDia1 by SwinA and unpolymerizable actins.

Within cells, the G-actin pool is regulated by a feedback mechanism that involves transcriptional upregulation of actin (Posern et al., 2002; Sotiropoulos et al., 1999). Autoregulation of actin transcription occurs via a mechanism in which G-actin binds MAL/MKL1, a coactivator of the serum-response factor (Miralles et al., 2003). In addition to this long-term transcriptional regulation of actin, our results add a short-term mechanism for generating actin polymers regulated by G-actin.

Our finding of G-actin regulation of mDia1-catalyzed actin nucleation prompted us to seek its relevance under physiological conditions. We discovered two insights into the regulation of mDia1 and other actin nucleators in homeostasis between G-actin and F-actin. First, the frequency of speckle appearance of mDia1Full and mDia1F2 correlates with the local concentration of AIP1, a cooperating molecule of the actin-depolymerizing factor, cofilin. G-actin released by fast actin turnover may therefore upregulate the efficiency of mDia1 locally. F-actin is also enriched around the foci for frequent mDia1 appearance. Cellular F-actin can exist at high concentrations: ~1000 μM in lamellipodia (Abraham et al., 1999) and >2000 μM in yeast actin patches (Wu and Pollard, 2005). The F-actin disassembly rate is fast (~0.03 second^{-1}) throughout lamellipodia (Watanabe and Mitchison, 2002). Therefore, G-actin may be released at a rate of ~30 μM/second and even faster around such foci. It takes a few seconds for G-actin to diffuse out of the local area (diffusion coefficient=3.1-5.8×10^{-8} cm^2/second) (McGrath et al., 1998). Together, these situations could lead to the formation of a local actin concentration gradient. We therefore postulate that either the locally high concentration of G-actin or the high ratio of G-actin to actin-sequestering proteins may result in frequent mDia1-catalyzed actin nucleation.

Second, we found that the G-actin increase induced by LatB triggers the formation of processive FRL1 and mDia1 speckles, but not speckles of the Arp2/3 complex. We propose that specific actin nucleators such as mDia1 and FRL1 sense G-actin within the range of free G-actin concentrations in cells. Dependency of nucleation on the G-actin concentration is different between Arp2/3 complex and formins in vitro; Arp2/3-complex-catalyzed nucleation appears to require a single actin monomer (Higgs et al., 1999), whereas formin-catalyzed nucleation occurs by stabilization of an actin dimer (Pring et al., 2003). Moreover, actin nucleation by the Arp2/3 complex also depends on preformed filaments and activators such as WASp/Scar proteins. Our data suggest that G-actin binding may not be a rate-limiting step in actin nucleation catalyzed by the Arp2/3 complex within cells. Further studies will help to elucidate differential regulation between actin nucleators by G-actin concentrations.

mDia1 demonstrates the greatest rate of accelerated actin elongation among the formin family (Kovar et al., 2006; Romero et al., 2004). Indeed, mDia1ΔN3 elongates actin at the rate of ~720 subunits/second in living cells (Higashida et al., 2004). Formin-bound barbed ends are protected from capping protein (Zigmond et al., 2003), which enables long-range actin elongation. The promotion of this F-actin-assembly mechanism is very rapid, because the increase in mDia1-catalyzed actin nucleation occurs several seconds after treatment with LatB. Cells whose diameter reach several tens of micrometers, may need rapid nucleation and fast elongation of F-actin when subjected to an actin-perturbing environment, such as exposure to mechanical stress. These properties of mDia1 may provide an efficient way to resist acute disruption of actin structures by rapidly restoring cellular actin polymers.

Materials and Methods

Plasmids and reagents

pEGFP-mDia1Full, ΔN3, F2 (Higashida et al., 2004), delCMV-EGFP-actin (Watanabe and Mitchison, 2002), delCMV-EGFP-p40 and delCMV-EGFP-CPβ1(Miyoshi et al., 2006) vectors were described previously. Point mutations in β-actin (G13R or R62D) were introduced in delCMV-EGFP-actin using PCR. Mutated β-actins were subcloned into the *Eco*RI and *Bam*HI site of p3xFLAG-CMV-7.1 (Sigma-Aldrich). Poly-L-lysine, cytochalasin D and a Flag M2 mouse monoclonal antibody were purchased from Sigma-Aldrich. Latrunculin B and jasplakinolide were from Calbiochem. Swinholide A was from Alexis Biochemicals. Texas-Red-X phalloidin and Alexa Fluor 594 goat anti-mouse IgG were from Invitrogen. The expression construct for mPlum-AIP1 was generated by fusing cDNA encoding a red fluorescent protein, mPlum (a gift from Roger Y. Tsien, University of California, San Diego, CA) and *Xenopus laevis* AIP1 cDNA (GenBank accession number, BC077202) obtained from IMAGE consortium. *Xenopus laevis* TPM (IMAGE 3403213) and FRL1 cDNA (GenBank accession number, BC074257) were from IMAGE consortium. The constructs for mPlum-mDia1ΔN3, TPM-EGFP and EGFP-FRL1 were generated by subcloning into appropriate vectors. Anti-Xac2 and anti-AIP1 antibodies were obtained by immunizing rabbits with recombinant proteins.

Live cell imaging and fluorescent microscopy

Speckle imaging and live cell imaging were carried out in XTC cells as described (Higashida et al., 2004; Miyoshi et al., 2006; Watanabe and Mitchison, 2002). Time-lapse imaging was performed using an Olympus BX52 microscope equipped with xenon illumination and a cooled CCD camera (Cool SNAP HQ, Roper Scientific), an Olympus BX51 microscope equipped with a cooled CCD camera (Cascade II:512, Roper Scientific) or Olympus inverted microscope, IX71, equipped with a cooled CCD camera (UIC-QE, Molecular Device). Speckle tracking was performed using Track Points in Metamorph software (Molecular Device). In drug perfusion experiments, time-lapse imaging was carried out intermittently by altering the acquisition intervals in order to track gradually slowing mDia1Full movement. Speckles moving in one direction for at least five consecutive frames at the speed of >0.05 μm/second were identified as processively moving speckles. The number of speckles was measured by counting the processive mDia1Full speckles that existed in one frame at the indicated time point if not stated. The measured cell areas are the same between before and after the treatment in each cell, but different between experiments.

LatB, CytD and jasplakinolide were dissolved in dimethylsulfoxide to produce stock solutions of 1 mM. Swinholide A was dissolved in methanol to produce a stock of 500 μM. All drugs were stored at –80°C. Diluted dimethylsulfoxide or methanol used during experiments did not exceed more than 0.3% in the medium and these concentrations did not affect the behavior of mDia1.

Measurement of Flag-actin experiments

In the experiments using mutant actins, cells were transfected with 1 μg pEGFP-mDia1Full and 8 μg p3xFLAG-actinWT, G13R or R62D. Cells were then seeded and cultured on coverslips for >20 hours. Time-lapse imaging was carried out in the presence of 10% FCS. Normalized frequency of processive mDia1 speckles was calculated as follows. The number of mDia1 speckles moving processively within a 10 second time window was counted and the data then normalized by dividing the speckle number by total intensity of EGFP fluorescence within the imaged region. Average intensity of EGFP fluorescence was within a 1.6-fold range between the three conditions (Fig. 2G).

Electroporation

Electroporation of C3 exoenzyme was performed as described (Kato et al., 2001). C3 (20 μg/ml) was electroporated into XTC cells ($0.8\text{-}1.5\times10^6$/ml) suspended in 75% Leibovitz's L15 medium containing 5% FCS.

Protein purification

E.coli strain BL21*trxB* (DE3) (Novagen) was transformed with the pGEX-4T-mDia1F2 construct (Higashida et al., 2004), and grown overnight at 37°C. After subculturing into fresh medium, cells were grown at 37°C for 3 hours, and then grown for 16 hours at 16°C with the addition of 0.1 mM isopropyl β-D-thiogalactopyranoside. Cells harvested by centrifugation were resuspended in buffer A [50 mM Tris-HCl pH 8.0, 500 mM NaCl, 5 mM EDTA,1 mM DTT and one tablet of complete protease inhibitor (Roche)], and sonicated. The sonicate was clarified at 50,000 ***g*** for 30 minutes, and mixed with glutathione-Sepharose (Amersham Biosciences) for 1 hour at 4°C. Sepharose was washed three times with an excess amount of buffer A without a protease inhibitor. Bound proteins were replaced in the buffer B (50 mM Tris-HCl pH 8.0, 0.1 mM $MgCl_2$, 100 mM NaCl, 10 mM $CaC1_2$, 1 mM DTT) and cleaved with thrombin protease (Amersham Biosciences) overnight at 4°C. Hirudin (Sigma) was added to inactivate the thrombin protease. Purified proteins were kept at 4°C. Human profilin I was expressed in *E. coli* and purified by poly-L-proline affinity chromatography.

Actin assembly assay

For the nucleation assay, actin stock (20% pyrene-labeled actin) was mixed in G buffer (2 mM Tris-HCl pH 8.0, 0.5 mM DTT, 0.2 mM ATP and 0.2 mM $CaCl_2$) and centrifuged at 150,000 ***g*** for 2 hours at 4°C. The supernatant was collected. Conversion to Mg^{2+} salts and induction of actin polymerization were performed as described previously (Li and Higgs, 2005). Pyrene fluorescence was monitored using Fluoroskan Ascent FL (Labsystems) in Fig.4A (excitation 355 nm, emission 405 nm) or Envision 2103 Multilabel Reader (Perkin Elmer) in supplementary material Fig. S4B (excitation 365 nm, emission 407 nm). In supplementary material Fig. S4A, experiments were performed as described previously (Suetsugu, S. et al., 2001) and pyrene fluorescence (excitation 365 nm, emission 407 nm) was monitored by FP-6500 (JASCO).

Quantification of free barbed ends

Quantification of free barbed ends was carried out as described previously (Miyoshi et al., 2006) with minor modifications including the use of Rhodamine-actin (Cytoskeleton) instead of recombinant CP-α2/EGFP-CPβ1. XTC cells were allowed to spread on PLL-coated glass coverslips for 40 minutes. Cells were permeabilized with 0.1% Triton-X 100 in cytoskeleton buffer (10 mM MES pH 6.1, 90 mM KCl, 3 mM $MgCl_2$, 2 mM EGTA, 0.16 M sucrose) plus 10 μM phalloidin (Sigma-Aldrich) for 10 seconds, and washed three times with buffer F' (10 mM Tris pH 7.5, 100 mM KCl, 2 mM $MgCl_2$, 1 mM ATP, 0.2 mM EGTA, 0.2 mM dithiothreitol, 1% bovine serum albumin) plus 10 μM phalloidin. Cells were incubated with Rhodamine-actin (10%, 0.5 μM) in buffer F' for 10 seconds, and washed three times with buffer F' supplemented with 10 μM phalloidin, 0.1 mg/ml glucose oxidase, 3 mg/ml glucose and 20 μg/ml catalase. Images were acquired within 10 minutes using an Olympus PlanApo 60× Oil Ph (NA 1.40).

We thank R. Y. Tsien for mPlum cDNA, C. Ampe for the human profilin I expression vector, T. Ishizaki and H. N. Higgs for help and suggestions in protein purification and D. Vavylonis for suggestions in simulation analysis. This work was supported in part by Grants-in-Aid for Scientific Research on Priority Areas from the Ministry of Education, Culture, Sport, Science and Technology of Japan. This work was also supported by grants from the Japan Science and Technology Corporation (S.S.) and grants from Uehara Memorial Foundation (N.W.). C.H. was a JSPS research fellow.

References

Abe, H., Obinata, T., Minamide, L. S. and Bamburg, J. R. (1996). Xenopus laevis actin-depolymerizing factor/cofilin: a phosphorylation-regulated protein essential for development. *J. Cell Biol.* **132**, 871-885.

Abraham, V. C., Krishnamurthi, V., Taylor, D. L. and Lanni, F. (1999). The actin-based nanomachine at the leading edge of migrating cells. *Biophys. J.* **77**, 1721-1732.

Brieher, W. M., Kueh, H. Y., Ballif, B. A. and Mitchison, T. J. (2006). Rapid actin monomer-insensitive depolymerization of Listeria actin comet tails by cofilin, coronin, and Aip1. *J. Cell Biol.* **175**, 315-324.

Bubb, M. R., Senderowicz, A. M., Sausville, E. A., Duncan, K. L. and Korn, E. D. (1994). Jasplakinolide, a cytotoxic natural product, induces actin polymerization and competitively inhibits the binding of phalloidin to F-actin. *J. Biol. Chem.* **269**, 14869-14871.

Bubb, M. R., Spector, I., Bershadsky, A. D. and Korn, E. D. (1995). Swinholide A is a microfilament disrupting marine toxin that stabilizes actin dimers and severs actin filaments. *J. Biol. Chem.* **270**, 3463-3466.

Buttery, S. M., Yoshida, S. and Pellman, D. (2007). Yeast formins Bni1 and Bnr1 utilize different modes of cortical interaction during the assembly of actin cables. *Mol. Biol. Cell* **18**, 1826-1838.

Coue, M., Brenner, S. L., Spector, I. and Korn, E. D. (1987). Inhibition of actin polymerization by latrunculin A. *FEBS Lett.* **213**, 316-318.

Evangelista, M., Zigmond, S. and Boone, C. (2003). Formins: signaling effectors for assembly and polarization of actin filaments. *J. Cell Sci.* **116**, 2603-2611.

Higashida, C., Miyoshi, T., Fujita, A., Oceguera-Yanez, F., Monypenny, J., Andou, Y., Narumiya, S. and Watanabe, N. (2004). Actin polymerization-driven molecular movement of mDia1 in living cells. *Science* **303**, 2007-2010.

Higgs, H. N., Blanchoin, L. and Pollard, T. D. (1999). Influence of the C terminus of Wiskott-Aldrich syndrome protein (WASp) and the Arp2/3 complex on actin polymerization. *Biochemistry* **38**, 15212-15222.

Hotulainen, P., Paunola, E., Vartiainen, M. K. and Lappalainen, P. (2005). Actin-depolymerizing factor and cofilin-1 play overlapping roles in promoting rapid F-actin depolymerization in mammalian nonmuscle cells. *Mol. Biol. Cell* **16**, 649-664.

Kato, T., Watanabe, N., Morishima, Y., Fujita, A., Ishizaki, T. and Narumiya, S. (2001). Localization of a mammalian homolog of diaphanous, mDia1, to the mitotic spindle in HeLa cells. *J. Cell Sci.* **114**, 775-784.

Kovar, D. R., Harris, E. S., Mahaffy, R., Higgs, H. N. and Pollard, T. D. (2006). Control of the assembly of ATP- and ADP-actin by formins and profilin. *Cell* **124**, 423-435.

Li, F. and Higgs, H. N. (2003). The mouse Formin mDia1 is a potent actin nucleation factor regulated by autoinhibition. *Curr. Biol.* **13**, 1335-1340.

Li, F. and Higgs, H. N. (2005). Dissecting requirements for auto-inhibition of actin nucleation by the formin, mDia1. *J. Biol. Chem.* **280**, 6986-6992.

Mabuchi, I., Hamaguchi, Y., Fujimoto, H., Morii, N., Mishima, M. and Narumiya, S. (1993). A rho-like protein is involved in the organisation of the contractile ring in dividing sand dollar eggs. *Zygote* **1**, 325-331.

Martin, S. G. and Chang, F. (2006). Dynamics of the formin for3p in actin cable assembly. *Curr. Biol.* **16**, 1161-1170.

McGrath, J. L., Tardy, Y., Dewey, C. F., Jr, Meister, J. J. and Hartwig, J. H. (1998). Simultaneous measurements of actin filament turnover, filament fraction, and monomer diffusion in endothelial cells. *Biophys. J.* **75**, 2070-2078.

Millonig, R., Salvo, H. and Aebi, U. (1988). Probing actin polymerization by intermolecular cross-linking. *J. Cell Biol.* **106**, 785-796.

Miralles, F., Posern, G., Zaromytidou, A. I. and Treisman, R. (2003). Actin dynamics control SRF activity by regulation of its coactivator MAL. *Cell* **113**, 329-342.

Miyoshi, T., Tsuji, T., Higashida, C., Hertzog, M., Fujita, A., Narumiya, S., Scita, G. and Watanabe, N. (2006). Actin turnover-dependent fast dissociation of capping protein in the dendritic nucleation actin network: evidence of frequent filament severing. *J. Cell Biol.* **175**, 947-955.

Ono, S. (2003). Regulation of actin filament dynamics by actin depolymerizing factor/cofilin and actin-interacting protein 1, new blades for twisted filaments. *Biochemistry* **42**, 13363-13370.

Otomo, T., Tomchick, D. R., Otomo, C., Panchal, S. C., Machius, M. and Rosen, M. K. (2005). Structural basis of actin filament nucleation and processive capping by a formin homology 2 domain. *Nature* **433**, 488-494.

Paul, A. S. and Pollard, T. D. (2008). The role of the FH1 domain and profilin in formin-mediated actin-filament elongation and nucleation. *Curr. Biol.* **18**, 9-19.

Pollard, T. D., Blanchoin, L. and Mullins, R. D. (2000). Molecular mechanisms controlling actin filament dynamics in nonmuscle cells. *Annu. Rev. Biophys. Biomol. Struct.* **29**, 545-576.

Posern, G., Sotiropoulos, A. and Treisman, R. (2002). Mutant actins demonstrate a role for unpolymerized actin in control of transcription by serum response factor. *Mol. Biol. Cell* **13**, 4167-4178.

Posern, G., Miralles, F., Guettler, S. and Treisman, R. (2004). Mutant actins that stabilise F-actin use distinct mechanisms to activate the SRF coactivator MAL. *EMBO J.* **23**, 3973-3983.

Pring, M., Cassimeris, L. and Zigmond, S. H. (2002). An unexplained sequestration of latrunculin A is required in neutrophils for inhibition of actin polymerization. *Cell Motil. Cytoskeleton* **52**, 122-130.

Pring, M., Evangelista, M., Boone, C., Yang, C. and Zigmond, S. H. (2003). Mechanism of formin-induced nucleation of actin filaments. *Biochemistry* **42**, 486-496.

Pruyne, D., Evangelista, M., Yang, C., Bi, E., Zigmond, S., Bretscher, A. and Boone, C. (2002). Role of formins in actin assembly: nucleation and barbed-end association. *Science* **297**, 612-615.

Ridley, A. J. and Hall, A. (1992). The small GTP-binding protein rho regulates the assembly of focal adhesions and actin stress fibers in response to growth factors. *Cell* **70**, 389-399.

Romero, S., Le Clainche, C., Didry, D., Egile, C., Pantaloni, D. and Carlier, M. F. (2004). Formin is a processive motor that requires profilin to accelerate actin assembly and associated ATP hydrolysis. *Cell* **119**, 419-429.

Rose, R., Weyand, M., Lammers, M., Ishizaki, T., Ahmadian, M. R. and Wittinghofer, A. (2005). Structural and mechanistic insights into the interaction between Rho and mammalian Dia. *Nature* **435**, 513-518.

Sagot, I., Rodal, A. A., Moseley, J., Goode, B. L. and Pellman, D. (2002). An actin nucleation mechanism mediated by Bni1 and profilin. *Nat. Cell Biol.* **4**, 626-631.

Sampath, P. and Pollard, T. D. (1991). Effects of cytochalasin, phalloidin, and pH on the elongation of actin filaments. *Biochemistry* **30**, 1973-1980.

Sotiropoulos, A., Gineitis, D., Copeland, J. and Treisman, R. (1999). Signal-regulated activation of serum response factor is mediated by changes in actin dynamics. *Cell* **98**, 159-169.

Suetsugu, S., Miki, H. and Takenawa, T. (2001). Identification of another actin-related protein (Arp) 2/3 complex binding site in neural Wiskott-Aldrich syndrome protein (N-WASP) that complements actin polymerization induced by the Arp2/3 complex activating (VCA) domain of N-WASP. *J. Biol. Chem.* **276**, 33175-33180.

Watanabe, N. and Mitchison, T. J. (2002). Single-Molecule Speckle Analysis of Actin Filament Turnover in Lamellipodia. *Science* **295**, 1083-1086.

Watanabe, N., Kato, T., Fujita, A., Ishizaki, T. and Narumiya, S. (1999). Cooperation between mDia1 and ROCK in Rho-induced actin reorganization. *Nat. Cell Biol.* **1**, 136-143.

Wu, J. Q. and Pollard, T. D. (2005). Counting cytokinesis proteins globally and locally in fission yeast. *Science* **310**, 310-314.

Yarmola, E. G., Somasundaram, T., Boring, T. A., Spector, I. and Bubb, M. R. (2000). Actin-latrunculin A structure and function. Differential modulation of actin-binding protein function by latrunculin A. *J. Biol. Chem.* **275**, 28120-28127.

Zigmond, S. H., Evangelista, M., Boone, C., Yang, C., Dar, A. C., Sicheri, F., Forkey, J. and Pring, M. (2003). Formin leaky cap allows elongation in the presence of tight capping proteins. *Curr. Biol.* **13**, 1820-1823.